Optical and magnetic properties of Fe^{2+} and Cr^{2+} in II-VI semiconductors: the Jahn-Teller effect

David Colignon [a], Eduard Kartheuser [a], Sergio Rodriguez [b], Murielle Villeret [c]

[a] *Institut de Physique B5, Université de Liège, B-4000 Liège, Belgium*
[b] *Department of Physics, Purdue University, West Lafayette, IN 47907-1396, USA*
[c] *Department of Mathematics, City University, London, EC1V 0HB, UK*

Abstract

The ^5D terms of Fe^{2+} and Cr^{2+} in the tetrahedral potential at cation sites in II-VI compounds split into orbital doublet and triplet states. While in Cr^{2+} the orbital triplet has lower energy than the doublet, the opposite is the case in Fe^{2+}. Both ions have singlet ground states after the spin-orbit interaction is taken into account and, hence, both are Van Vleck paramagnets. The optical absorption spectra of Fe and Cr based materials differ and are explained on the basis of a *dynamic* Jahn-Teller effect in the former and a *static* one in the latter. These considerations permit us to explain the optical as well as the magnetic properties observed in these materials.

1. Introduction

We study the Jahn-Teller effect on the optical and magnetic properties of Fe^{2+} and Cr^{2+} in the tetrahedral potential at cation sites in II-VI semiconductors. Both the iron and the chromium-based materials are Van Vleck paramagnets. The effective Hamiltonian of one of these ions is:

$$H = H_0 + V_c(T_d) + \lambda \boldsymbol{L} \cdot \boldsymbol{S} - \rho\left[(\boldsymbol{L} \cdot \boldsymbol{S})^2\right.$$
$$\left. + \tfrac{1}{2}\boldsymbol{L} \cdot \boldsymbol{S} - \tfrac{1}{3}L(L+1)S(S+1)\right] + H_{J-T}, \quad (1)$$

where H_0 is the Hamiltonian of the free ion omitting the spin-orbit interaction $\lambda L \cdot S$ and the spin-spin interaction [1], λ and ρ are respectively the strength of the spin-orbit interaction and the spin-spin interaction, L and S are the orbital and spin angular momenta of the ion. Fig. 1 shows the splitting of the ^5D term of the free ions for both Fe^{2+} (a) and Cr^{2+} (b) according to the Hamiltonian (1) (the static Jahn-Teller effect included for Cr^{2+}). The wave functions used are described by Colignon et al. [2].

Crystal field theory accounts for the general features of the excitation spectrum but fails to provide an explanation for the spacing of the energy levels in the $^5\Gamma_3$ and $^5\Gamma_5$ multiplets of Fe^{2+} and Cr^{2+}. We note that the absolute value of the free ion spin-orbit strength λ is larger in Fe^{2+} than in Cr^{2+}. As a result, we show that the Jahn-Teller interaction H_{J-T} overcomes the spin-orbit interaction $\lambda L \cdot S$ in the latter.

2. Optical and magnetic properties of Fe^{2+} based II-VI compounds

The authors have recently presented a theoretical model [2] accounting for the positions and oscillator strengths of the optical absorption lines in the near [3] and far [4] infrared in $CdTe:Fe^{2+}$. Starting from the spin-orbit wave functions appropriate to the energy level scheme of Fig. la , we constructed the symmetry-adapted vibronic basis associated with phonons of symmetries Γ_3 and Γ_5 involved in the dynamic Jahn-Teller Hamiltonian H_{J-T} of Eq. (1). Using this basis, the calculated eigenvalues and eigenvectors of the Hamiltonian operator in Eq. (1) are then fitted to the available optical data. Phonon overtones up to $n = 6$ for the Γ_3 phonon and up to $n = 10$ for the Γ_5 phonon were included to ensure convergence of the energy values of the vibronic states.

Agreement between theory and experiment was obtained with the following parameters: $^5\Gamma_3$-$^5\Gamma_5$ orbital splitting $\Delta = 2529.9$ cm^{-1}, $\lambda = -95$ cm^{-1}, $\rho = 0.7$ cm^{-1} and Jahn-Teller interaction $E_{J-T}^{(5)} = 275$ cm^{-1} in the excited state and

$E_{J-T}^{(3)} = 1.97$ cm^{-1} in the ground state describing coupling between the localized 3d electrons and phonons of energies $\hbar\omega_5 = 40$ cm^{-1} and $\hbar\omega_3 = 28$ cm^{-1} of symmetries Γ_5 and Γ_3, respectively.

Fig. 1. *Schematic drawing of the energy levels of Fe^{2+} and Cr^{2+} at a cation site in II-VI compounds having zinc blende (T_d) structure with crystal field parameters Δ. (a) : Spin-orbit split levels of Fe^{2+}. (b): Static Jahn-Teller model of Cr^{2+} with Jahn-Teller energy E_{J-T} and spin-orbit level spacing D.*
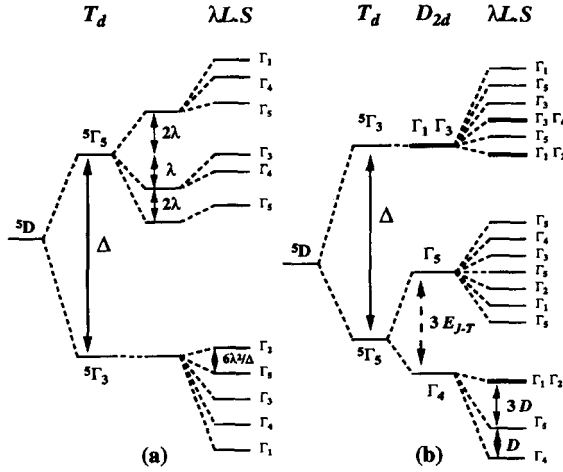
In the presence of an external magnetic field B the Zeeman interaction $\mu_B(L + 2S)\cdot B$ mixes the states in Fig. 1 giving rise to a paramagnetic susceptibility χ of the Van Vleck type (μ_B is the Bohr magneton); χ for Fe^{2+} in CdTe is isotropic but, at high magnetic fields ($B > 15$ T), when the magnetization M ceases to be linear in B, there is a noticeable anisotropy [5], the maxima and minima of $|M|$ occurring when B points along a cubic axis and a $\langle 111 \rangle$ direction, respectively. This has been shown [6] using similar material parameters but disregarding the Jahn-Teller coupling. The dynamic Jahn-Teller effect, altering mainly the upper $^5\Gamma_5$ multiplet does not modify the order of the magnetization curves. These findings are in qualitative agreement with experiments [5]. We conclude that the available optical and magnetic data for CdTe:Fe^{2+} are well explained by crystal field theory invoking a dynamic Jahn-Teller coupling.

3. Optical and magnetic properties of chromium-based II-VI compounds

Despite the great similarities with iron-based II-VI compounds, the optical data of chromium-based semiconductors cannot be explained by means of the same theoretical model and assuming only a reversal of the orbital doublet with the orbital triplet. EPR [7] and optical absorption data [8,9] are consistent with a strong static tetragonal (D_{2d}) Jahn-Teller distortion. This situation can be described by assuming that this static Jahn-Teller interaction is smaller than the crystal field splitting Δ but larger than the spin-orbit interaction (see Fig. 1b). Using this model and $\lambda = 58$ cm^{-1}, we obtain the material parameters given in Table 1 from a fit of the numerical diagonalization of the 25×25 Hamiltonian (1) to experiment. Notice that in contrast to results obtained by others [9-11], we have used the free ion value λ for chromium in our fitting procedure, instead of relying on the measurements [8,9] of the Jahn-Teller energy in the ground state orbital triplet. The static Jahn-Teller distortion in the $^5\Gamma_3$ orbital excited state has been neglected here in agreement with references [7] and [8].

Table 1. *Crystal field parameter Δ, ground state Jahn-Teller energy E_{J-T} and spin-spin parameter p obtained from the zero-phonon line v [8] and EPR data (D) [7]*

| Material	D (cm^{-1})	v (cm^{-1})	Δ (cm^{-1})	E_{J-T} (cm^{-1})	ρ (cm^{-1})
CdTe	+ 0.26	4700	4346	278	0
ZnTe	2.3	4994	4837	113	0
ZnSe	-2.48	4975	4604	340	0.716

It has been shown from our numerical analysis and from a perturbation calculation that for a fixed value of λ, the

physical parameter D (see Fig. 1b) is very sensitive to the Jahn-Teller energy E_{J-T} in the ground state and to the spin-spin parameter ρ. For instance, for ZnSe ($D < 0$) a decrease in p leads to a larger Jahn-Teller energy whereas in the case of ZnTe and CdTe ($D > 0$), $\rho > 0$ would even further decrease the Jahn-Teller energy.

Having determined the physical parameters from the optical data, we analyze recent measurements of the magnetic properties of chromium-based II-VI compounds, the magnetic specific heat and the magnetization [10,11]. We have shown [6] that the theoretical model developed for the iron-based materials (see Fig. 1a with reversed level scheme) cannot account for the measured low field ($B < 6$ T) anisot-ropy of the magnetization for different orientations of B. Fig. 2 shows the magnetic specific heat per Cr ion as a function of temperature at $B = 0$, obtained with the material parameters of Table 1. The difference in behavior of this physical quantity clearly reflects the reversal of the level scheme in the ground state multiplet of Cr^{2+} in ZnSe as compared to that in CdTe and ZnTe, i.e. the sign and magnitude of the physical parameter D. As shown in Fig. 2, the theoretical results are in good agreement with the existing data for $Zn_{1-x}Cr_xSe$ [10] and $Zn_{1-x}Cr_x$ Te [11], but low temperature (< 3 K) measurements are not available to confirm the predicted spike in the magnetic specific heat in this temperature range.

Fig. 2. *Magnetic specific heat per chromium ion of $Zn_{1-x}Cr_xTe$, $Zn_{1-x}Cr_rSe$ and $Zn_{1-x}Cr_xTe$ as a function of temperature and in absence of magnetic field (experimental data taken from [10] and [11]).*
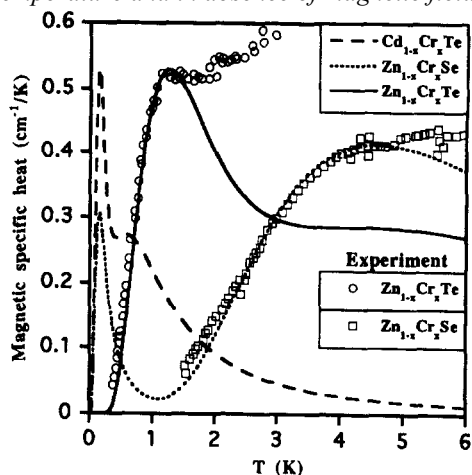
Fig. 3. *Anisotropy of the magnetization in $Zn_{,1-x}Cr_xTe$ at 3.65 K and $Cd_{1-x}Cr_x$ Te at 0.5 K for three orientations of the magnetic field with respect to the cubic axes of the crystal and for a concentration $x = 0.004$ (experimental data taken from [11]).*
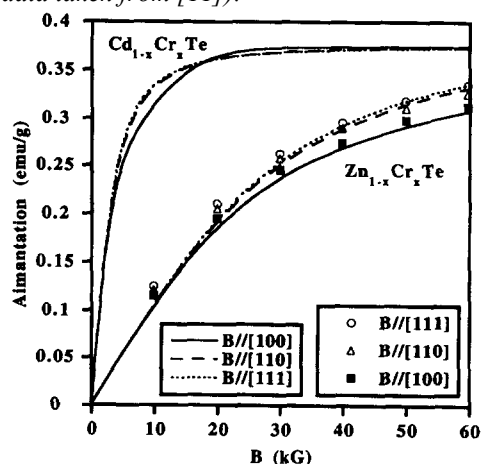
The macroscopic magnetization is a statistical average of the contributions resulting from the three Jahn-Teller distortions along the (100) cubic axes. These distortions are inequivalent at finite magnetic field intensity. Fig. 3 shows the magnetization assuming equal numbers of these distortions. The results of calculations of the

magnetization in $Zn_{1-x}Cr_xTe$ at 0.5 K and in $Zn_{1-x}Cr_xTe$ at 3.65 K are shown as a function of the intensity B for three different orientation of B. We note that the non-equilibrium situation (Fig. 3) seems to describe rather well the experimental data for $Zn_{1-x}Cr_xTe$. This is in agreement with results by Pekarek et al. [11], including the corrections to the spin-orbit interaction due to the mixing with ligand p orbitals. The theoretical results for $Zn_{1-x}Cr_xTe$ have been displayed at 0.5 K because in this case the structure of the ground state multiplet ($D = 0.26$ cm^{-1}) leads to a nearly isotropic behavior of the magnetization as a function of magnetic field orientation. Experimental data are not available for $Zn_{1-x}Cr_xTe$.

The results of our analysis show that the optical and magnetic data of iron and chromium based II-VI compounds can be understood within the framework of crystal field theory including coupling between the 3d electrons and the phonons of the host crystal.

References

[1] A. Abragam and B. Bleaney, Electron Paramagnetic Resonance of Transition Ions (Clarendon, Oxford, 1970) p. 398.

[2] D. Colignon, E. Kartheuser, S. Rodriguez and M. Villeret, Phys. Rev. B 51 (1995) 4849.

[3] M.K. Udo, M. Villeret, I. Miotkowski, A.J. Mayur, A.K. Ramdas and S. Rodriguez, Phys. Rev. B 46 (1992) 7459.

[4] C. Testellin, C. Rigaux, A. Mauger, A. Mycielski and C. Julien, Phys. Rev. B 46 (1992) 2183.

[5] C. Testellin, C. Rigaux, A. Mauger, A. Mycielski and M. Guillot, Phys. Rev. B 46 (1992) 2193.

[6] E. Kartheuser, S. Rodriguez and M. Villeret, Phys. Rev. B 48 (1993) 14127.

[7] J.T. Vallin and G.D. Watkins, Phys. Rev. B 9 (1974) 2051.

[8] J.T. Vallin, G.A. Slack, S. Roberts and A.E. Hughes, Phys. Rev. B 2 (1970) 4313.

[9] M. Kaminska, J.M. Baranowski, S.M. Uba and J.T. Vallin, J. Phys. C 12 (1979) 2197.

[10] W. Mac, A. Twardowski, P.J.T. Eggenkamp, H.J.M. Swagten, Y. Shapira and M. Demianiuk, Phys. Rev. B 50 (1994) 14144.

[11] T.M. Pekarek, J.E. Luning, I. Miotkowski and B.C. Crooker, Phys. Rev. B 50 (1994) 16914.